

Metal-insulator transition in the mixed-valence manganites

L. Sheng

Department of Physics and Texas Center for Superconductivity, University of Houston, Houston, Texas 77204

D. Y. Xing

*Department of Physics and Texas Center for Superconductivity, University of Houston, Houston, Texas 77204
and National Laboratory of Solid State Microstructures, Nanjing University, Nanjing 210093, China*

D. N. Sheng and C. S. Ting

*Department of Physics and Texas Center for Superconductivity, University of Houston, Houston, Texas 77204
(Received 22 July 1997)*

It is found that the sharp resistivity peak observed near the Curie temperature T_C in the manganites $R_{1-x}A_x\text{MnO}_3$ is closely correlated to the residual resistivity ρ_0 of the sample, suggesting that nonmagnetic randomness plays an important role in determining their anomalous properties. Using the one-parameter scaling theory to study the electronic localization due to both the nonmagnetic randomness and the double exchange spin disorder, we show that the sharp resistivity peak is caused by the Anderson metal-insulator (M-I) transition and that $\rho_0 > \rho_c$ (a critical value) is a prerequisite to the occurrence of the M-I transition. T_C as a function of ρ_0 has also been calculated. These results are in good agreement with experimental measurements. [S0163-1829(97)51836-4]

The mixed-valence oxides $R_{1-x}A_x\text{MnO}_3$ (where $R=\text{La, Nd, Pr}$; $A=\text{Ca, Sr, Ba, Pb}$) have recently been subjected to intense experimental¹⁻¹⁰ and theoretical¹¹⁻¹⁸ investigations because of a huge negative magnetoresistance (colossal magnetoresistance or CMR) exhibited in samples of $0.2 < x < 0.5$. For such a range of doping, the resistivity ρ vs temperature T curve usually exhibits a sharp peak at a certain temperature T_p , indicating a crossover from metallic behavior ($d\rho/dT > 0$) below T_p to activated behavior ($d\rho/dT < 0$) above T_p . The application of an external magnetic field strongly suppresses ρ and moves the resistivity peak to higher temperatures, thereby producing a CMR near T_p . It is generally accepted that the anomalous transport phenomena in these $R_{1-x}A_x\text{MnO}_3$ systems are closely related to their magnetic properties, in particular the paramagnetic (PM)-ferromagnetic (FM) phase transition upon cooling. Most experimental measurements¹⁻¹⁰ indicate that T_p is very close to the Curie temperature T_C , which is reminiscent of the double exchange (DE) model¹⁹ based on the exchange of electrons between Mn^{3+} and Mn^{4+} ions.

For the Mn oxides, metallic ferromagnetism occurs in the composition range $0.2 < x < 0.5$, where it is associated with the simultaneous presence of Mn^{3+} and Mn^{4+} ions. Each Mn^{3+} ion has four $3d$ electrons, three in the t_{2g} state and the fourth in the e_g state. The Hund's rule coupling is very strong so that spins of all the d electrons on a given site must be parallel. Three t_{2g} electrons are localized on the Mn site and give rise to a local spin S of magnitude $3/2$, while the e_g electron may hop into the vacant e_g states of surrounding Mn^{4+} ions. Owing to the strong Hund's rule coupling, the hopping of an e_g electron between Mn^{3+} and Mn^{4+} sites is affected by the relative alignment of the local spins, being maximal when the localized spins are parallel and minimal when they are antiparallel. The sharp drop in ρ below T_C can be attributed to the fact that an increase in the magnetization

M upon cooling should reduce spin disorder scattering and thus increase the carrier conductivity. However, whether DE alone can account for the anomalous transport behavior is a question at issue.^{13,16,17}

By using a simplified DE Hamiltonian, a perturbative calculation¹³ of ρ near T_C is found to disagree with experimental results by an order of magnitude or more, wherefore extra physics such as strong Jahn-Teller-type coupling between electrons and lattice was proposed as a necessary extension. Theoretical attempts^{14,15} to incorporate the DE effects and the strong electron-phonon interaction led to the suggestion that there is a crossover from a Fermi liquid to a small polaron regime in which the conduction is dominated by the hopping motion of self-trapped polarons. This theory predicted¹⁴ a sharp peak in the ρ vs T curve at half-filling ($x=0$) but failed to get a large magnetoresistance in combination with metallic low T behavior in doped samples. On the other hand, authors in Refs. 16 and 17 recently pointed out that the e_g electrons would acquire a nontrivial phase when they move in closed loops, and this effect might favor electronic localization in the DE model. However, such a qualitative suggestion still lacks the support of quantitative studies.

It is widely accepted that there is a close correlation between the resistivity peak and the FM-PM transition. After inspecting experimental data,¹⁻¹⁰ we find that both of them are associated with the residual resistivity $\rho_0 = \rho(T=0)$ of the samples. A high residual electrical resistivity appears to be a prerequisite to the occurrence of the sharp resistivity peak near T_C ;³ there is no obvious resistivity peak in relatively clean samples ($\rho_0 < 10^{-4} \Omega \text{ cm}$). At the same time, the Curie temperature T_C is observed to be higher for clean samples and lower for dirty ones. Since ρ_0 , in the FM ground state, arises from the nonmagnetic randomness rather than spin disorder, the correlations mentioned above strongly sug-

gest that nonmagnetic randomness plays a significant role in determining the transport and magnetic properties of the Mn oxides.

In this paper we propose that the nonmagnetic randomness together with the spin disorder leads to an Anderson metal-insulator (M-I) transition near T_C , from which the anomalous properties of transport and magnetism in the Mn oxides can be well understood. Using the well-established scaling theory,²⁰ we study the electronic localization by considering diagonal disorder and off-diagonal disorder. The former is introduced to describe the nonmagnetic randomness, and the latter comes from the DE model including the nontrivial phase.^{16,17} We find that the off-diagonal disorder alone can only localize a small fraction of electron states close to the band edges but fails to cause localization of the electron states at the Fermi level for intermediate hole doping. Our scaling calculations show that, in the presence of a suitable strength of nonmagnetic disorder, the spin disorder frozen in at the FM-PM transition will cause the localization of electrons at the Fermi surface and induce a M-I transition near T_C in the doping range of $0.2 < x < 0.5$. In order to find the correlation between ρ_0 and the M-I transition as well as the FM-PM transition, we evaluate the residual resistivity necessary for observing the M-I transition and the Curie temperature T_C as a function of ρ_0 . The calculated results are found to be well consistent with experimental observations.

The Hamiltonian used to describe the Mn oxides is

$$H = - \sum_{ij} \tilde{t}_{ij} d_i^\dagger d_j + \sum_i \varepsilon_i d_i^\dagger d_i. \quad (1)$$

Here the first term is the DE Hamiltonian of e_g electrons, in which \tilde{t}_{ij} is the effective transfer integral between nearest-neighbor Mn sites. It was proposed recently¹⁶ that \tilde{t}_{ij} has the form

$$\tilde{t}_{ij} = t \left\{ \cos\left(\frac{\theta_i}{2}\right) \cos\left(\frac{\theta_j}{2}\right) + \sin\left(\frac{\theta_i}{2}\right) \sin\left(\frac{\theta_j}{2}\right) \exp[-i(\varphi_i - \varphi_j)] \right\}, \quad (2)$$

with t the transfer integral in the absence of the Hund's rule coupling and (θ_i, φ_i) the polar angles characterizing the orientation of local spin \mathbf{S}_i . Since the scaling behavior of localization is well-known to be universal, i.e., independent of details of the disorder, we can use the diagonal disorder [the second term in Eq. (1)] to represent the total effect due to all possible nonmagnetic disorders, where ε_i is the random on-site energy. The nonmagnetic disorders in the Mn oxides may mainly come from the doping of A^{2+} , which leads to a local random potential fluctuation and lattice distortion. Here, we have neglected the superexchange interaction between localized spins, which should be small compared with the electron kinetic energy in the intermediate doping range. In the FM state at low temperatures, where all the localized spins are aligned (M reaches its maximum value), $\tilde{t}_{ij} \equiv t$ and so the randomness only comes from the second term of Eq. (1). As temperature is increased, the contribution of the off-diagonal disorder to the electronic localization increases, along with the gradual disorder of the spin orientations.

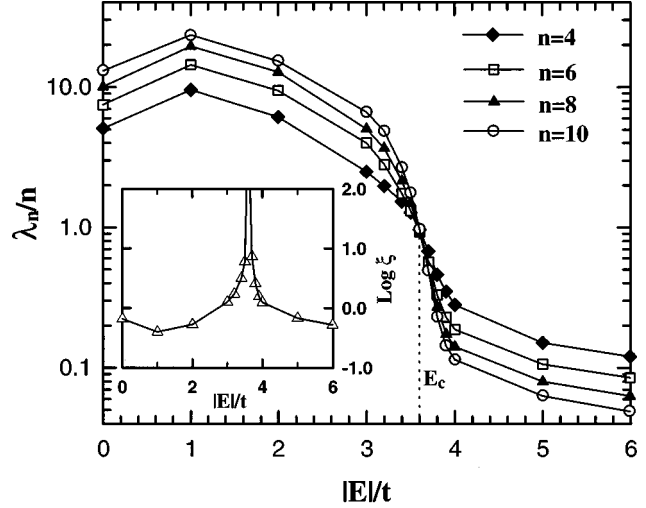


FIG. 1. The renormalized finite-size localization length λ_n/n as a function of the dimensionless energy $|E|/t$. Inset: logarithm of the scaling parameter ξ as a function of $|E|/t$.

When the system enters into PM phase ($M=0$), the random \tilde{t}_{ij} gives maximal off-diagonal disorder.

The localization calculations are performed in two steps according to the one-parameter scaling theory.²⁰ First, consider a three-dimensional bar of an essentially infinite length $L=10^5$ and a finite cross-section $n \times n$ (the lattice constant a being taken to be unity) and evaluate its localization length by calculating the system Lyapunov exponents for the transfer matrix. Second, the localization length in the $n \rightarrow \infty$ limit is obtained by means of a finite-size scaling analysis.

Let us study first the localization effect in the DE model in the absence of diagonal disorder ($\varepsilon_i=0$). In this case, all electron states in the e_g band are extended in the FM phase by the lack of disorder. For the PM phase, $\cos\theta_i$ and φ_i are taken as independent variables that are uniformly distributed in regions $[-1, 1]$ and $[-\pi, \pi]$, respectively, corresponding to a complete random distribution of the spin orientation.¹⁷ Figure 1 shows the calculated localization length λ_n as a function of energy $|E|$ on the bars with $n=4, 6, 8$, and 10 . Note that all the curves are crossed at a fixed point E_c . To go to the infinite-size limit, we fit the calculated λ_n/n to the universal one-parameter scaling function²⁰

$$\frac{\lambda_n(E)}{n} = F\left(\frac{n}{\xi(E)}\right). \quad (3)$$

The scaling parameter $\xi(E)$ is found to have two branches (see the inset of Fig. 1), an indication that there are localized and extended states in the e_g band. For $|E| > E_c$, $\lambda_n(E)/n$ decreases toward zero with increasing n , so we expect the localization length $\lambda_n(E)$ to converge to a finite value for $n \rightarrow \infty$ and identify $\xi(E)$ with the localization length $\lambda_\infty(E)$ for an infinite system. For $|E| < E_c$, $\lambda_n(E)/n$ increases with n , and so λ_n diverges as $n \rightarrow \infty$, where $\xi(E)$ becomes a correlation length of the electrons. It follows that E_c is the mobility edge separating the localized states at $|E| > E_c$ from the extended states at $|E| < E_c$. The present calculation yields $E_c \approx 3.6t$. In the range of hole concentration $0.2 < x < 0.5$, the Fermi level is within the region of $2t > E_F > 0$, where $E_F = 0$

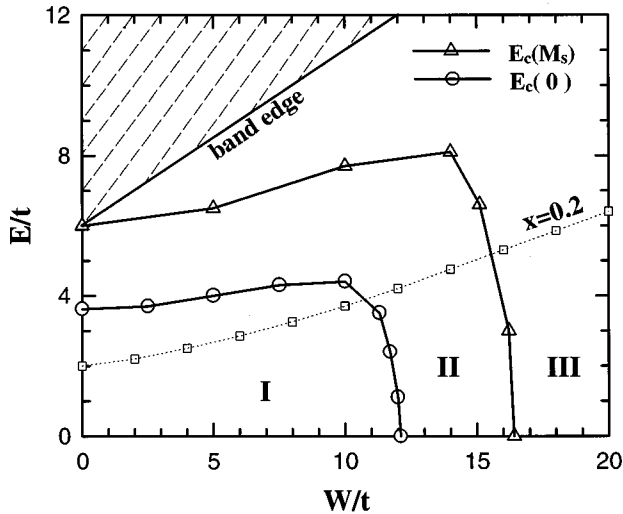


FIG. 2. Phase diagram in the E/t vs W/t plane. Opened triangles represent the calculated mobility edge in the FM state, circles stand for the mobility edge in the PM state, and small squares on the light dotted line are the Fermi energy corresponding to hole concentration $x=0.2$. The lower half of the conduction band with $E<0$ is not shown here.

corresponds to a Fermi level at the center of the band. Thus, under the present frozen-spin approximation, the DE spin disorder is found to be not able to localize the carriers on the Fermi surface.

Next we take both off-diagonal and diagonal disorder into account by assuming ε_i to be uniformly distributed within $[-W/2, W/2]$, and evaluate, respectively, the mobility edges $E_c(M=M_s)$ for the FM state in the absence of the off-diagonal disorder and $E_c(M=0)$ for the PM state in the presence of the off-diagonal disorder. Here M_s represents the magnetization for completely aligned spins. Figure 2 shows the calculated results of $E_c(M_s)$ (opened triangles) and $E_c(0)$ (opened circles) as functions of the diagonal disorder W . The dotted line with small squares stands for the Fermi level E_F in the FM state for $x=0.2$, which is evaluated by diagonalizing the Hamiltonian of $10 \times 10 \times 10$ cubic lattice with periodic boundary conditions and averaging the corresponding density of states over 100 set values of the random variables. For the hole concentration of $0.2 < x < 0.5$, E_F lies between the dotted line and the $E=0$ axis. It is found from our calculation that the change of the Fermi level from the FM to PM state is smaller than $0.4t$ in this doping range. By making a comparison between $E_c(0)$ and $E_c(M_s)$, we find that for fixed W the off-diagonal disorder shifts the mobility edge toward the band center ($E=0$) and hence increases the proportion of localized states in the conduction band. There is a critical magnitude W_c at which all the electron states in the conduction band become localized. It decreases from $W_c(M_s) \approx 16.5t$ to $W_c(0) \approx 12t$ as the off-diagonal disorder is switched on.

For a given system, the disorder parameter W and the Fermi energy E_F are approximately unchanged, corresponding to a point in the phase diagram of Fig. 2. However, the mobility edge varies with temperature since the spin disorder is temperature dependent. With the system changing from the FM ground state at $T=0$ to the PM state at $T>T_C$ on

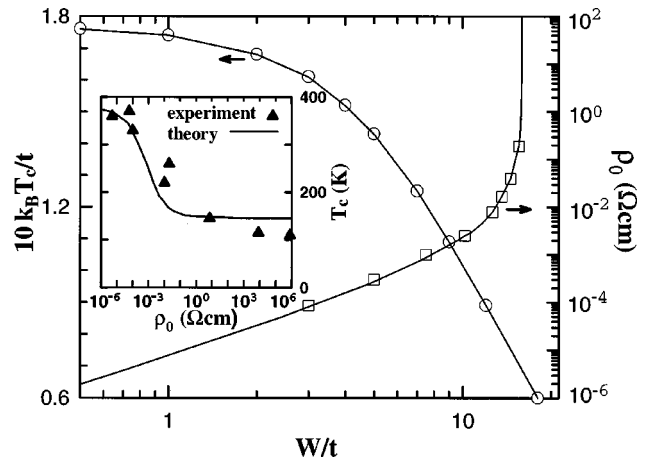


FIG. 3. Calculated residual resistivity ρ_0 and Curie temperature T_C as functions of diagonal disorder parameter W/t . Inset: comparison between the theoretical result for T_C vs ρ_0 and experimental data.

warming, the mobility edge should change continuously from $E_c(M_s)$ to $E_c(0)$. The phase diagram is divided into three regions by the mobility edges $E_c(M_s)$ and $E_c(0)$, and one can identify different conduction behaviors according to which region the point (W, E_F) lies in. If (W, E_F) is in region I, the system always exhibits metallic behavior in both the FM and PM states; while if it is in region III, the system always exhibits insulatorlike behavior. For (W, E_F) in region II, the system will undergo an Anderson M-I transition that is intimately related to the FM-PM phase transition. Such a transition is of particular interest since it is associated with the sharp resistivity peak observed in the Mn oxides. We can expect that the M-I transition temperature T_p should be very close to the Curie temperature T_C , where the magnetization decreases sharply from $M \approx M_s$ to $M=0$. In the range of $0.2 < x < 0.5$, relatively strong disorder $12t < W < 16.5t$ is necessary to make the M-I transition occur.

In order to compare the theory with experimental data for the Mn oxides $R_{1-x}A_x\text{MnO}_3$, we now calculate the residual resistivity ρ_0 and the Curie temperature T_C . The calculation of ρ_0 due to relatively strong nonmagnetic disorder W needs a nonperturbative approach, and the Landauer formula is suitable for this case. By using the Landauer formula together with the scaling analysis, ρ_0 is related to the scaling parameter $\xi(E)$ as $\rho_0 = (2h/e^2)\xi a$.²⁰ The resistivity ρ_0 as a function of W/t calculated for $x=0.3$ is shown as opened squares in Fig. 3, where the lattice constant is taken to be $a=4.0 \text{ \AA}$ as a reasonable value for the Mn oxides.⁷ The solid curve is the best fit to the calculated results, where the power laws $\rho_0 \propto W^2$ (Born approximation) and $\rho_0 \propto (W_c - W)^{-1.3}$ (Ref. 21) have been considered, respectively, in the extrapolations of $W \rightarrow 0$ and $W \rightarrow W_c \approx 16t$. To determine T_C , we compare the system free energy in the FM state with that in the PM state. When the system changes from the PM to FM state, the e_g electrons can hop more freely and hence lower their kinetic energy by $\Delta \bar{E} = \bar{E}_{PM} - \bar{E}_{FM}$, where the average energy is given by $\bar{E}_a = \int dE D_a(E) E f(E - \mu_a)$ with $a = \text{FM, PM}$. Here, the density of states $D_a(E)$ is calculated by finite-size diagonalization and the chemical potential μ_a in the Fermi-Dirac dis-

tribution function $f(E - \mu_a)$ is determined from the condition of fixed hole concentration $1 - x = \int dE D_a(E) f(E - \mu_a)$. On the other hand, the entropy loss of the localized spins increases the free energy by $k_B T \ln(2S+1)$ per site, so the Curie temperature is determined approximately by $\Delta \bar{E} = k_B T_C \ln(2S+1)$. The obtained $k_B T_C$ scaled by t for different W are also given in Fig. 3 (opened circles). One sees that T_C decreases with increasing diagonal disorder W . This is easily understood from the fact that the disorder resists electronic motion and so disfavors DE ferromagnetism. Combining the W dependence of ρ_0 and that of T_C given in Fig. 3, we readily obtain T_C as a function of ρ_0 . A comparison between the present theoretical results and the experimental data of Coey *et al.*⁷ is shown in the inset of Fig. 3, where the hopping integral is taken to be $t = 0.19$ eV, a reasonable value for the Mn oxides corresponding to a bandwidth of 2.3 eV.¹⁷ The theoretical values of T_C , even when the disorder is small, are in good agreement with experiments. Our results are somewhat different from those obtained by Millis,¹³ but are very close to those estimated by Varma.¹⁷

From the ρ_0 vs W relation given in Fig. 3, it is found that the critical value $W \approx 12t$ corresponds to $\rho_0 = \rho_c \sim 10^{-3} \Omega \text{ cm}$ and $W \approx 16t$ corresponds to $\rho_0 \rightarrow \infty$. It then follows that the Anderson M-I transition will occur when the condition $\rho_0 > \rho_c$ is satisfied. In this case, the resistivity $\rho(T)$ exhibits metallic behavior below $T_p (= T_C)$, having a positive temperature coefficient. Above T_p , the conduction carriers are localized and the resistivity is governed by the variable range hopping,^{17,20} leading to insulatorlike behavior with a negative temperature coefficient. This transition behavior disappears for $\rho_0 \ll \rho_c$. Experimental measurements show that most Mn oxides conform to the rule predicted above. Figure 2 of Ref. 7 gives systematical experimental data for the Mn oxides $R_{0.7}A_{0.3}MnO_3$ with ρ_0 ranging from

5×10^{-6} to $8 \times 10^5 \Omega \text{ cm}$. We can see that the upper four ρ vs T curves with ρ_0 above ρ_c all exhibit sharp peaks near T_C ; while the lower two curves with ρ_0 well below ρ_c have no evident peak. In the crossover region between the two cases mentioned above, where ρ_0 is smaller than but close to ρ_c , the Anderson transition does not occur, but strong electronic quantum interference among scatters (weak localization effect) still exists above T_C . This effect may result in a slow decrease in the resistivity with T (Ref. 20) in the PM state and a low peak of resistivity near T_C . As a result, we conclude that $\rho_0 > \rho_c$, for which the Anderson M-I transition can occur, is the optimum condition for observing the sharp resistivity peak and the associated CMR in the Mn oxides.

In summary it is proposed that the nonmagnetic randomness and the effective hopping disorder in the double exchange model play a dominant role in determining the anomalous transport property and the magnetism in the Mn oxides. Using the one-parameter scaling theory, we have studied the electronic localization by considering the diagonal and off-diagonal disorder and found that, in the presence of suitable nonmagnetic disorder, an Anderson metal-insulator transition will follow the ferromagnetic-paramagnetic transition. The residual resistivity and T_C are calculated as functions of the strength of the nonmagnetic disorder. Our theoretical results can well account for the essential features of experimental observations in Mn oxides. Finally, we wish to point out that the dynamical aspect of the DE model has been neglected in our calculation. It is believed¹⁷ that this dynamical effect should not change the qualitative behavior of the results obtained from the present frozen-spin approximation.

This work was supported by the Texas Center for Superconductivity at the University of Houston, and by the Robert A. Welch foundation. D.Y.X. was also supported by the National Natural Science Foundation of China.

¹R. M. Kusters *et al.*, *Physica B* **155**, 362 (1989).

²R. von Helmolt *et al.*, *Phys. Rev. Lett.* **71**, 2331 (1993).

³S. Jin *et al.*, *Science* **264**, 413 (1994).

⁴Y. Tokura *et al.*, *J. Phys. Soc. Jpn.* **63**, 3931 (1994); A. Asamitsu *et al.*, *Nature (London)* **373**, 407 (1995).

⁵J. I. Neumeier *et al.*, *Phys. Rev. B* **52**, R7006 (1995).

⁶P. Schiffer *et al.*, *Phys. Rev. Lett.* **75**, 3336 (1995).

⁷J. M. D. Coey *et al.*, *Phys. Rev. Lett.* **75**, 3910 (1995).

⁸P. G. Radaelli *et al.*, *Phys. Rev. Lett.* **75**, 4488 (1995).

⁹J. Fontcuberta *et al.*, *Phys. Rev. Lett.* **76**, 1122 (1996).

¹⁰R. Mahendiran *et al.*, *Phys. Rev. B* **53**, 3348 (1996).

¹¹N. Furukawa, *J. Phys. Soc. Jpn.* **63**, 3214 (1994).

¹²J. Inoue and S. Maekawa, *Phys. Rev. Lett.* **74**, 3407 (1995).

¹³A. J. Millis, P. B. Littlewood, and B. I. Shraiman, *Phys. Rev. Lett.* **74**, 5144 (1995).

¹⁴A. J. Millis, B. I. Shraiman, and R. Mueller, *Phys. Rev. Lett.* **77**, 175 (1996).

¹⁵H. Roder, J. Zang, and A. R. Bishop, *Phys. Rev. Lett.* **76**, 1356 (1996).

¹⁶E. Müller-Hartmann and E. Dagotto, *Phys. Rev. B* **54**, R6819 (1996).

¹⁷C. M. Varma, *Phys. Rev. B* **54**, 7328 (1996).

¹⁸J. Jiang, J. Dong, and D. Y. Xing, *Phys. Rev. B* **55**, 8973 (1997).

¹⁹C. Zener, *Phys. Rev.* **82**, 403 (1951); P. W. Anderson and H. Hasegawa, *ibid.* **100**, 675 (1955); P. -G. de Gennes, *ibid.* **118**, 141 (1960).

²⁰A. Mackinnon and B. Kramer, *Phys. Rev. Lett.* **47**, 1546 (1981); *Z. Phys. B* **53**, 1 (1983).

²¹E. Hofstetter and M. Schreiber, *Phys. Rev. B* **49**, 14726 (1994).